4 Search for Cold Dark Matter Particles with XENON

A. Askin, L. Baudis, A. Ferella, M. Haffke, A. Kish, A. Manalaysay, R. Santorelli, E. Tziaferi

In collaboration with: Columbia, INFN, LLNL, Brown, CWRU, Coimbra, Rice, Yale

(XENON Collaboration)

Dark matter detectors based on liquid noble elements (Ar, Xe) are rapidly evolving and are providing sensitivities comparable to the ones of cryogenic mK-experiments. The best prospects for the unambiguous identification of a Weakly Interacting Massive Particle (WIMP) lie in detectors having negligible background competing with the dark matter signal. This can be achieved by using nuclear recoil discrimination in order to veto competing electron recoil events, by effective neutron shielding, and through the operation of a large homogeneous detector volume with 3-D position resolution. The latter information can be used to select single hit events characteristic of a WIMP interaction while rejecting multiple hit events associated with backgrounds that propagate from the edge of the detector into the fiducial volume. In order to achieve an increase in scattering rate sensitivity to $\sigma \sim 10^{-46}\mathrm{cm}^2$ (10^{-10}pb) a fiducial target mass on the order of 1 ton will be required which will yield $\sim$10 events per year. An increase in target mass alone is not sufficient, unless the competing backgrounds are eliminated. Efficient and redundant background rejection schemes are thus a key requirement for any WIMP experiment, along with the capability to observe nuclear recoil energy depositions as low as a few keV. Liquid argon (LAr) and xenon (LXe) have excellent properties as dark matter targets. They are intrinsic scintillators, with high scintillation (λ = 128 nm for Ar, λ = 178 nm for Xe) and ionization yields. They are available in large quantities and can be purified to 1 ppt (parts per trillion)-levels. Scintillation in LAr and LXe is produced by the formation of excimer states, which are bound states of ion-atom systems. If a high electric field ($\sim$1 kV/cm) is applied, ionization electrons can also be detected, either directly or through the secondary process of proportional scintillation. Measuring both the primary scintillation signal and a secondary process yields a method of discriminating between electron and nuclear recoils. Our group is involved in the 3-phased XENON project. The first phase, XENON10, has been successfully operated at the Gran Sasso Underground Laboratory (LNGS) and has provided the most stringent limits on spin-independent and spin-dependent, pure-neutron, WIMP-nucleon cross sections. XENON100 is currently being commissioned at LNGS, while the first studies for the next step, XENON1t, have been started.

4.1 The XENON10 and XENON100 experiments

The XENON10 detector was a 15 kg active mass, dual-phase (liquid and gas) xenon time projection chamber, operated in WIMP search mode at LNGS from August 2006 to February 2007. It used two arrays of UV-sensitive photomultipliers (PMTs) to detect the prompt and proportional light signals induced by particles interacting in the sensitive liquid xenon (LXe) volume. The bottom array of 41 PMTs was located below the cathode, fully immersed in LXe, and mainly detected the prompt light signal. The 48 PMTs of the top array were located in the cold gas above the liquid, detecting the proportional light signal

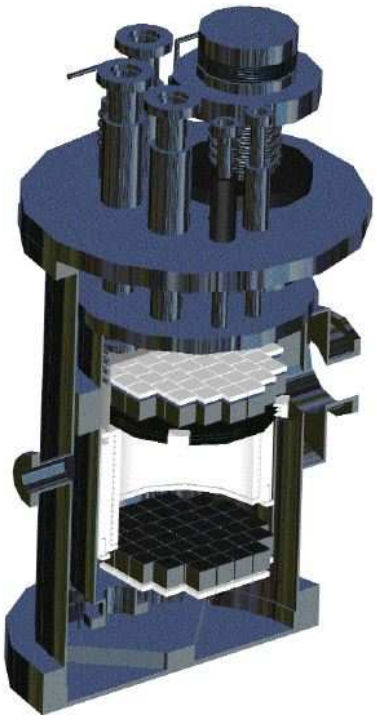

Figure 4.1: A schematic view XENON10 time projection chamber. Two UV-sensitive PMT arrays are used to detect the scintillation light produced by particles interacting in the 15 kg of active liquid xenon mass.

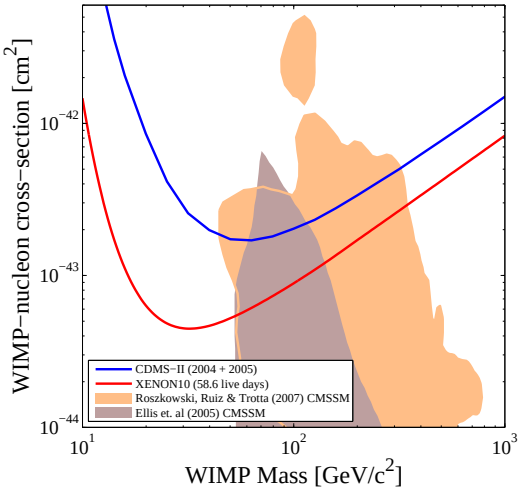

Figure 4.2: Limits on the Spin-Independent WIMP-nucleon cross section from XENON10 (red). Also shown are the CDMS-II 2005 result (blue) and theoretical predictions from supersymmetric models (filled regions).

which is created by the collision of extracted electrons with Xe atoms in the gas phase (the drift field was 1 kV/cm). Figure 4.1 shows a schematic view of the detector. The experiment had been calibrated with external gamma (^{57}Co, ^{137}Cs), an AmBe neutron source and with a small amount of neutron activated Xe gas, allowing a uniform energy and position calibration across the LXe active volume. The two Xe meta-stable states, ^{131m}Xe and ^{129m}Xe decay with 164 keV and 236 keV gamma rays with half-lives of 11.8 and 8.9 days, respectively. XENON10 had full 3D position sensitivity: the time separation between the two pulses of direct and proportional light (with a of maximum 75 μs) provided the event depth of an interaction with $<$1 mm resolution, the hit pattern in the top PMT array providing the x-y position with a resolution of a few mm.

The XENON10 results, using $\sim$136 kg-days exposure after cuts, demonstrated that LXe can be used for stable, homogeneous, large scale dark matter detectors, providing excellent position resolution and discrimination against the electron recoil background. The derived upper bound on the SI cross section on nucleons is 4.5 $\times 10^{-8}$pb for a WIMP mass 30 GeV/c^2. Figure 4.2 shows the SI limit as a function of WIMP mass, along with theoretical predictions for the neutralino. Since natural Xe contains ^{129}Xe (26.4%) and ^{131}Xe (21.2%) isotopes, each of these having an unpaired neutron, the XENON10 results substantially constrain the SD WIMP-nucleon cross section.

Our group was involved in several aspects for XENON10, such as measurements of the light yield with a small LXe prototype, material screening with a high-purity Ge detector in a new low-background facility at LNGS, Monte Carlo geometry of the detector and simulations of the gamma, alpha and neutron backgrounds, calibrations with n and γ sources, data processing and analysis as well as operations at LNGS. Some of these will be highlighted in the following sections.

Figure 4.3: The XENON100 TPC, fully assembled. The PTFE structures for the TPC and PMT holder were built at the UZH Physik Institut.

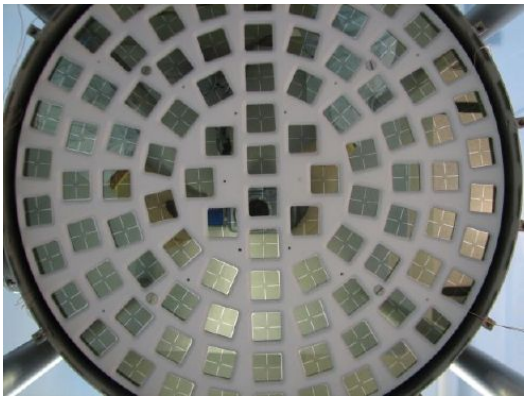

Figure 4.4: A picture of the XENON100 top PMT array with 98 square, UV-sensitive PMTs.

The 100 kg scale experiment, XENON100, is presently being commissioned at LNGS. Figure 4.3 shows a picture of the assembled inner structure. A picture of the top PMT array is shown in Fig. 4.4. XENON100 will operate a total of 170 kg (70 kg fiducial) of xenon, viewed by 242 PMTs, in a dual-phase TPC in an improved XENON10 shield. While the fiducial mass is increased by more than a factor of 10, the background will be lower by about a factor of 100 (through careful selection of ultra-low background materials, the placing of cryogenic devices and high-voltage feedthroughs outside of the shield and by using 100 kg of active LXe shield) compared to XENON10. The aim is to start the first science run in fall 2008, probing WIMP-nucleon SI cross sections down to $\sim 2 \times 10^{-9}$ pb.

The main activities of our group are testing and calibrations of XENON100 PMTs, material screening with the HPGe detector, Monte Carlo geometry, simulations of backgrounds and light collection efficiency simulations, energy calibrations with various sources, production of the inner TPC structures, as well as commissioning, operations, data processing and analysis.

4.2 Measurement of the liquid Xenon scintillation yield from low-energy nuclear recoils

When particles interact in LXe, they produce prompt scintillation photons and ionized electrons. The *yield*, defined as the number of quanta produced per unit energy, depends on the particle species interacting in the medium. The XENON10 experiment (1) has pushed the energy threshold of LXe detectors down to values where the yield for nuclear recoils is poorly understood. This lack of knowledge was the largest source of systematic uncertainties for the XENON10 results. In LXe dark matter experiments the energy scale of particle interactions is determined by the scintillation signal, thus the relevant quantity is not the full yield, but the scintillation yield of nuclear recoils. The low-energy electronic recoil energy scale is in general calibrated by using the photo-absorption line of 122 keV gammas from ^{57}Co.

The scintillation yield of nuclear recoils relative to the scintillation yield of 122 keV gammas is known as $\mathcal{L}_{eff}$. We have recently measured $\mathcal{L}_{eff}$ at the Radiological Research Accelerator Facility (RARAF) at Columbia University (in collaboration with the Columbia group). In previous measurements the behavior of $\mathcal{L}_{eff}$ at higher energies was flat at approximately 0.19, while more recent measurements suggested that below 20 keV $\mathcal{L}_{eff}$ departed from this (2; 3) value. Our new results from the measurement at the RARAF, shown in Fig. 4.5, tested $\mathcal{L}_{eff}$ down to 5 keV nuclear recoil energies and is not in agreement with previous results at these low energies. A publication of our results and their implication for the XENON10 dark matter limits is in progress.

Another quantity of interest for LXe dark matter detectors is the ionization yield of nuclear recoils at low energies. First measurements down to 20 keV exist (4); however the energy threshold of XENON10 was 4.5 keV and extrapolations from higher energies were necessary. To perform new, lower energy measurements using a mono-energetic neutron beam, a dedicated dual phase xenon time projection chamber is currently being constructed at the Physik Institut.

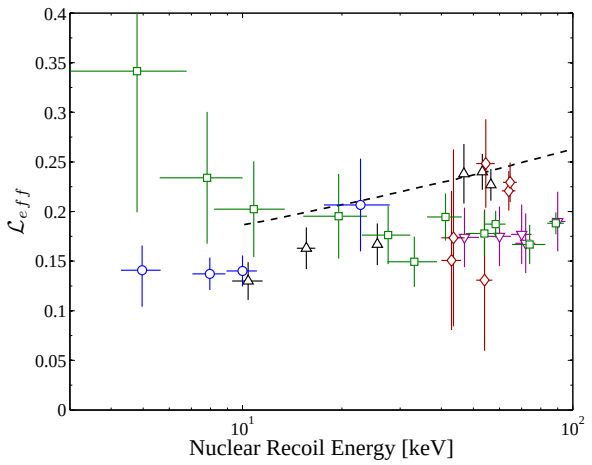

Figure 4.5: Recent measurements of $\mathcal{L}_{eff}$. Symbols correspond to (○)–this work; (□)–Chepel et al. [3]; (△)–Aprile et al. [2]; (◊)–Akimov et al. [6]; (▽)–Arneodo et al. [5]. Also shown is the theoretical prediction from Hitachi (dashed line) [7].

4.3 Material screening with a HPGe detector in a new low-background facility

To understand the residual radioactivity of materials and shields in terms of their U, Th, K and Co contaminations and model the expected backgrounds of the XENON experiments, we have installed an ultra-low background, high purity germanium detector (GATOR) at LNGS. A picture of the detector in its completed low-background shield is shown in Fig. 4.6.

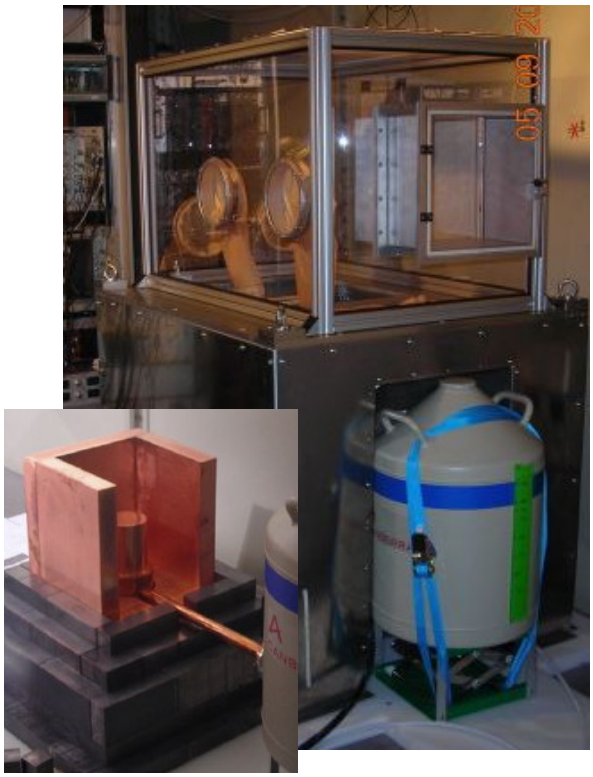

Figure 4.6: The HPGe detector in its completed shield structure at LNGS. The inset shows the detector in its open low-background Cu and Pb shield structure.

In Fig. 4.7 we show the comparison between the background of GATOR in its new facility, in its old shield at the Soudan Lab along

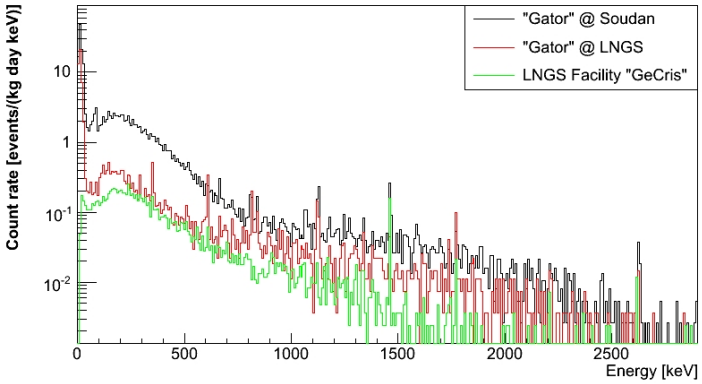

Figure 4.7:
Background spectra of Gator at Soudan (black), of Gator at Gran Sasso (red) and of a high purity germanium detector at Gran Sasso screening facility.

with the background of one of the world's most sensitive HPGe detectors, operated at LNGS. The background of GATOR is thus comparable to best existing HPGe detectors, and it will further improve with the decay of cosmogenic activities with typical half-lifes of 1 year.

To calculate GATOR's efficiency for each screening sample and to understand the detector's residual backgrounds we have implemented its detailed geometry into GEANT4. We have simulated ^{238}U, ^{232}Th, ^{60}Co, ^{40}K decays inside the copper cryostat and shield, ^{54}Mn, ^{65}Zn, ^{57}Co, ^{60}Co decays (cosmogenic nuclides) inside the Ge crystal and the Cu, as well as residual ^{222}Rn decays inside the N_2-purged sample chamber. An optimization of the background model is currently in progress.

We have screened several XENON10 and XENON100 materials (a subset of results are shown in Table 4.1) and have identified low-background materials, such as the stainless steel used for the cryostat and the high-voltage grids.

4.4 Gamma and neutron background studies for XENON100

The GATOR screening results are used to predict the gamma- and neutron-induced backgrounds in XENON100, which are mainly caused by the natural radioactive contamination of detector materials and shields. We have coded the detailed detector geometry in GEANT4 (a picture is shown in Fig. 4.8) and have simulated the main background contributions. The total predicted gamma background for XENON100 (shown in Fig. 4.9) in the WIMP search energy region (4.5 keV–30 keV) is at the level of 10×10^{-3} events/(kg day keV), before the yield based background discrimination. The breakdown of the different contributions is shown in table 4.2.

Table 4.1: **A subset of materials screened with the GATOR HPGe detector installed at LNGS.**

Material	Unit	^{238}U [mBq/unit]	^{232}Th [mBq/unit]	^{40}K [mBq/unit]	^{60}Co [mBq/unit]
PMT bases	base	0.71 ± 0.05	0.10 ± 0.03	NA	NA
22 PMTs	PMT	< 0.240	0.18 ± 0.05	11.5 ± 2.0	0.55 ± 0.1
12 PMTs	PMT	< 0.13	0.13 ± 0.05	13 ± 2	0.7 ± 0.1
Poly (I)	kg	2.426	< 0.674	< 4.658	< 0.536
Poly (II)	kg	< 3.80	< 2.69	< 5.88	< 0.684
S. Steel	kg	3.6 ± 0.8	1.8 ± 0.5	7 ± 1	< 4.92

We have also simulated the neutrons from spontaneous fission of ^{238}U and (α,n) reactions in the XENON100 detector and shield materials. Table 4.3 shows the resulting rates, with a total rate of $\sim 3 \times 10^{-6}$ events/(kg day keV) averaged over the 4.5 keV–30 keV energy region. Figure 4.10 shows the expected WIMP spectrum for a WIMP mass of 100 GeV/c^2 and a WIMP-nucleon cross-section of 2×10^{-45} cm^2, along with the predicted neutron background spectrum.

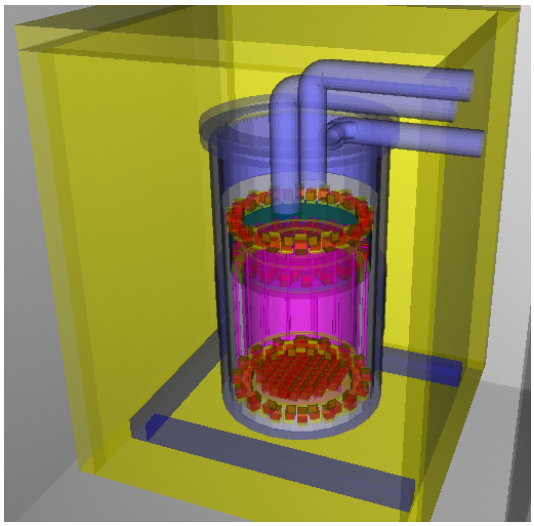

Figure 4.8: Geant4 geometry of the XENON100 detector and the inner shield.

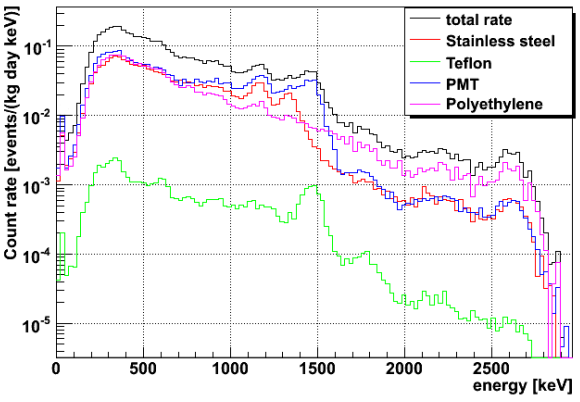

Figure 4.9: Predicted gamma background for XENON100, using measured residual radioactivity values for the detector and shield materials.

Table 4.2: Predicted gamma background rate in the WIMP search energy region (4.5 keV–30 keV) of XENON100.

Material	Rate of single scatters (10^{-3}events/(kg day keV))
Stainless Steel	2.01 ± 0.22
Teflon	0.68 ± 0.04
PMT	4.91 ± 0.60
Polyethylene	3.09 ± 0.29
Copper	0.026 ± 0.002
Total	10.72 ± 0.69

Table 4.3: Predicted neutron background rate in the WIMP search energy region (4.5 keV–30 keV) of XENON100.

Material	Rate of single nuclear recoils (10^{-7}events/(kg day keV))
Stainless Steel	2.93 ± 0.03
PMTs	3.18 ± 0.02
Teflon	6.26 ± 0.08
Copper	0.11 ± 0.02
Lead	0.38 ± 0.02
Polyethylene	4.87 ± 0.10
Liquid Xenon	1.07 ± 0.01
Total	28.8 ± 0.20

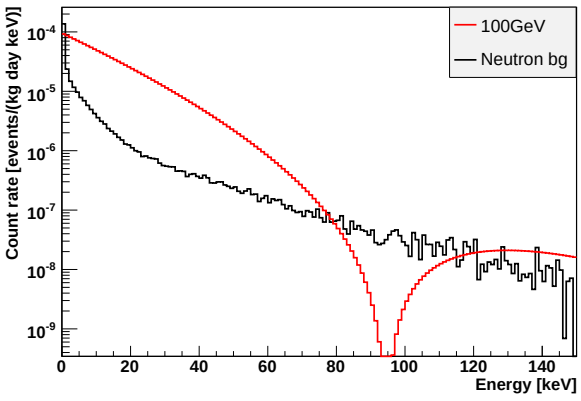

Figure 4.10: Predicted total neutron background (black) and expected WIMP spectrum (red) for a WIMP mass of 100 GeV/c^2 and a WIMP-nucleon cross-section of 2×10^{-45} cm^2.

An additional source of (high-energy) neutrons are interactions of fast cosmic muons with the rock and the Pb shield surrounding the detector. The angular distribution and energy spectrum of muons at the Gran Sasso Laboratory depth is known, and was used in propagating muons through a few meters of rock and into the XENON100 shields and detector. These simulations are currently in progress; the rate of single neutron interactions in the active volume is however expected to be lower than the one from the radioactivity of materials. Apart from background simulations, we are responsible for simulating the calibration sources ($^{57}_{27}$Co, $^{60}_{27}$Co, $^{137}_{55}$Cs, $^{228}_{90}$Th, Am-Be) and for light collection efficiency simulations and position reconstruction via neuronal network techniques.

4.5 Tests of XENON100 UV-sensitive photomultipliers

In order to determine the functionality of the PMTs used for XENON100 (Hamamatsu R8520), a PMT test facility was built at LNGS. The main aim of the test was to check each PMT before being placed inside the detector, rejecting poorly working devices, and selecting the best devices in terms of various parameters. The PMTs have been listed according to their measured gain, peak to valley ratio, resolution on single electrons and quantum efficiency (QE); the best PMTs have been selected to be placed in the most critical locations. In order to maximize the light detection of the tiny primary signal, the PMTs with highest QE have been placed on the bottom array. The PMTs showing the best single electron spectrum (in terms of the peak to valley ratio and resolution) have been placed in the outer ring of the top array where the position resolution, based on the analysis of the proportional light pattern, has to be precisely determined. More than 200 PMTs (in batches of 6) have been tested in a custom built black box containing a blue LED. The PMT signals have been integrated through a charge preamplifier and amplified through a shaping amplifier, before being acquired by a MCA. For each PMT several spectra were recorded according to different amounts of light stimulation (from 1 phe to some hundreds of phe's) and supplied voltage (from 650 V to 900 V).

In addition, the PMTs have been tested before and after having been kept for 48 h in dry ice in order to check their capability to work at cryogenic temperatures and to detect any noticeable change in their performance. From all the tested PMTs, 20 demonstrated a slightly worse performance and have been kept as spares, while 14 have been returned to the factory because of bad single electron response or failures after the cooling test.

[1] J. Angle et al. (XENON Collaboration), Phys. Rev. Lett. **100**, 021303 (2008).

[2] E. Aprile et al., Phys. Rev. D **72**, 072006 (2005).

[3] V. Chepel et al., Astropart. Phys. **26**, 58 (2006).

[4] E. Aprile et al., Phys. Rev. Lett. **97**, 081302 (2005).

[5] F. Arneodo et al., Nucl. Inst. and Meth. A **449**, 147 (2000).

[6] D. Akimov et al., Phys. Lett. B **524**, 245 (2002).

[7] A. Hitachi, Astropart. Phys. **24**, 247 (2005).

[8] J. Angle *et al.* [XENON10 Collaboration], Phys. Rev. Lett. **100** 021303 (2008).

[9] G.Carugno et al., Nucl. Inst. and Met. **A292** 580-584 (1990).